GS2018-5

Geochemistry, Sm-Nd isotopes and U-Pb geochronology of volcanic rocks from the North Star assemblage and the West Reed–North Star shear zone, Flin Flon belt, west-central Manitoba (parts of NTS 63K10, 15): implications for VMS prospectivity

by S. Gagné, S.D. Anderson, M. Hamilton[1], R.-L. Simard and M. Lazzarotto[2]

In Brief:

- The North Star assemblage represents a package of bimodal volcanic and volcaniclastic rocks with an arc-signature that has distinct geochemical and Sm-Nd isotopic characteristics
- A new U-Pb zircon age of 1895.9 ±1.6 Ma for a rhyolite from the North Star assemblage is similar in age to the main VMS-hosting volcanic sequences from the Flin Flon and Snow Lake areas
- The Rail deposit is interpreted to be part of the North Star assemblage

Citation:
Gagné, S., Anderson, S.D., Hamilton, M., Simard, R.-L. and Lazzarotto, M. 2018: Geochemistry, Sm-Nd isotopes and U-Pb geochronology of volcanic rocks from the North Star assemblage and the West Reed–North Star shear zone, Flin Flon belt, west-central Manitoba (parts of NTS 63K10, 15): implications for VMS prospectivity; *in* Report of Activities 2018, Manitoba Growth, Enterprise and Trade, Manitoba Geological Survey, p. 48–63.

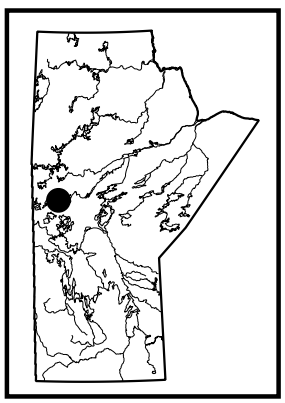

Summary

The West Reed–North Star shear zone (WRNS), traceable over a distance of 38 km west and northwest of Reed Lake in the Flin Flon belt, consists of layered tectonites hundreds of metres thick. The tectonites mark the boundary between two packages of bimodal volcanic and volcaniclastic rocks that host volcanogenic massive sulphides (VMS). The well-documented volcanic-arc/arc-rift rocks of the Fourmile Island assemblage (FIA) lie east of the WRNS and occur continuously along the entire trace of the WRNS. West of the WRNS lies another package of bimodal arc/arc-rift volcanic and volcaniclastic rocks termed the 'North Star assemblage' (NSA). The NSA is exposed along two main stretches separated by a 10 km gap. Geochemical investigation of the NSA rocks indicates that the northern and southern segments of the NSA are part of the same arc assemblage but have a complex volcanic history that includes generation of enriched mid-ocean ridge basalt (E-MORB), tholeiites with weak arc signatures and bimodal transitional to calc-alkaline magmatism. The distinct geochemical signatures of the NSA and FIA are both recognized in tectonized rocks within the WRNS. The Rail VMS deposit, interpreted to be located entirely within the WRNS, is hosted by rocks with a geochemical character similar to that of the NSA. Trace element signatures and Sm-Nd isotopic data show that NSA volcanism represents a more evolved sequence of juvenile-arc rocks, fed by a deeper magmatic source, compared to arc-volcanic rocks of the FIA.

Rhyolite at North Star Lake has been dated at 1895.9 +/-1.6 Ma and, considering it represents a significant volume of the NSA rocks, it is interpreted that the bulk of the arc assemblage was emplaced around 1896 Ma.

Introduction

Paleoproterozoic rocks in the Reed Lake area (Figure GS2018-5-1) are a component of a larger tectonic collage of volcano-plutonic and sedimentary rocks assembled during the closure of an ancient ocean (ca. 1.9–1.8 Ga) and collectively termed the 'Flin Flon belt' (FFB). The FFB contains numerous base-metal VMS deposits and is among the world's most prolific VMS districts (Syme et al., 1999). In the Reed Lake area and to the south beneath Phanerozoic sedimentary rocks, the FFB has significant potential to host additional VMS deposits. Despite the presence of several economic deposits, including the Reed Cu-Zn mine which ceased production in August 2018 after having depleted its reserves (Figure GS2018-5-1), the geological setting of VMS deposits in the Reed Lake area is not well understood. Previous workers recognized that significant stratigraphic, geochemical and isotopic differences exist between arc-volcanic rocks in the Flin Flon (Amisk collage) and Snow Lake areas, which suggested that these two segments of the FFB formed in distinct tectonic settings (Stern et al., 1995a; Lucas et al., 1996). Moreover, the Reed Lake area includes some major structural zones that resulted from the complex assembly of the FFB.

[1] Department of Earth Sciences, University of Toronto, 22 Russell Street, Toronto, ON M5S 3B1
[2] Department of Geosciences, University of Calgary, 2500 University Drive NW, Calgary, AB T2N 1N4

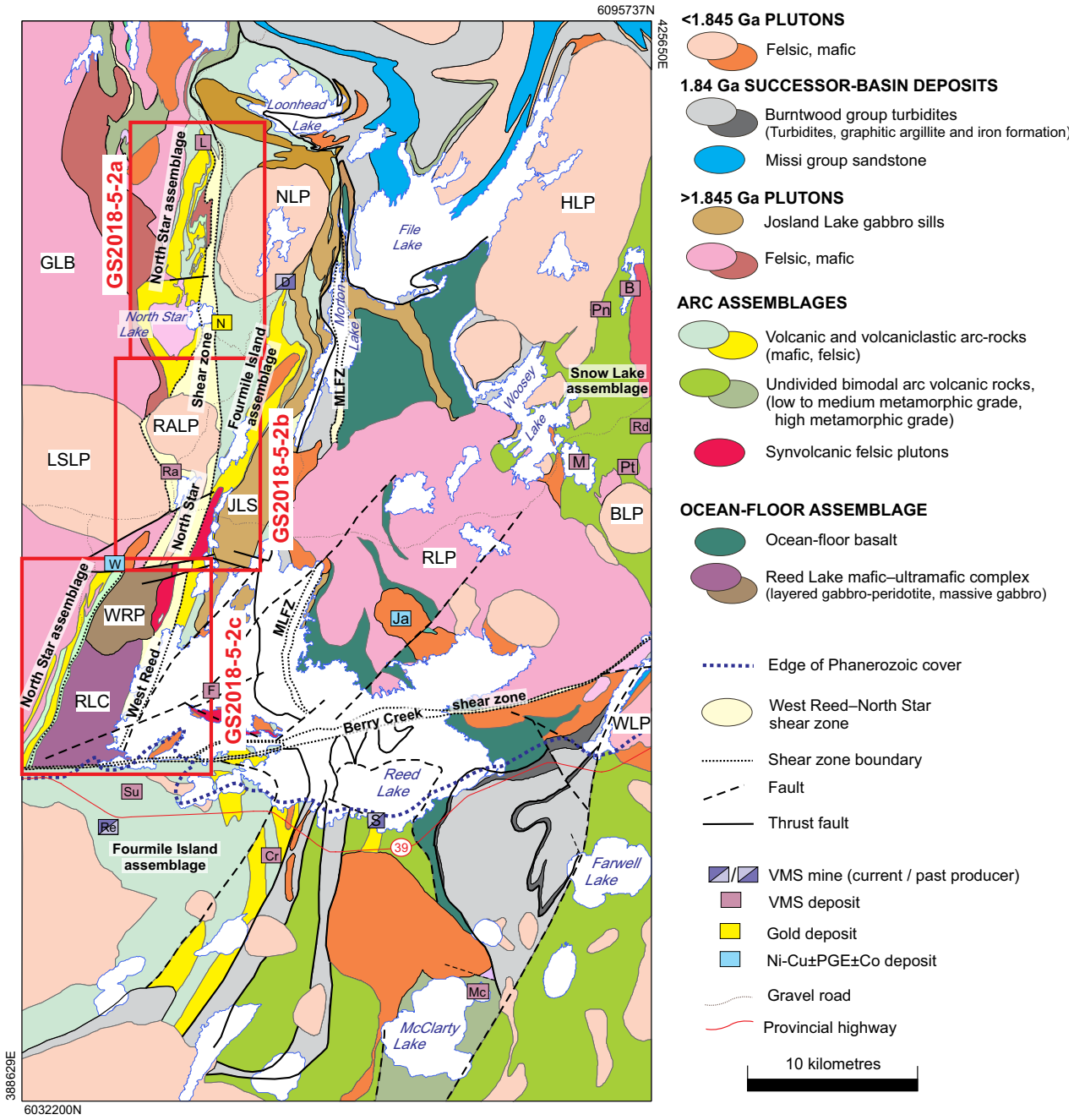

Figure GS2018-5-1: *Generalized geology of the Reed Lake area (compiled from Syme et al., 1995a; NATMAP Shield Margin Project Working Group, 1998; Gagné, 2017; Gagné et al., 2017). Intrusive rocks: BLP, Bujarsky Lake pluton; GLB, Gants Lake batholith; HLP, Ham Lake pluton; JLS, Josland Lake sills; LSLP, Little Swan Lake pluton; NLP, Norris Lake pluton; RALP, Rail Lake pluton; RLC, Reed Lake mafic–ultramafic complex; RLP, Reed Lake pluton; WLP, Wekusko Lake pluton; WRP, West Reed pluton. Structural feature: MLFZ, Morton Lake fault zone. Mines (active or closed), deposits and significant mineral occurrences: B, Bomber; Cr, Cowan River zone; D, Dickstone; F, Fourmile Island; Ja, Jackfish; L, Lon; M, Morgan; Mc, McClarty; N, North Star; Pn, Pen; Pt, Pot; Ra, Rail; Rd, Raindrop; Re, Reed; S, Spruce Point; Su, Super Zone; W, Wine. Other abbreviations: PGE, platinum-group elements; VMS, volcanogenic massive sulphide. Co-ordinates are in UTM Zone 14 (NAD83).*

One of these major structures, hundreds of metres wide, is the WRNS, which consists of tectonized mafic and felsic rocks that separate two sequences of bimodal volcanic rocks (Figure GS2018-5-1) that host VMS deposits. Rocks of the FIA occupy the eastern margin of the WRNS (Bailes, 1980; Syme et al., 1995b; Zwanzig and Bailes, 2010; Gagné, 2013; Gagné and Anderson, 2014a). Along the western margin of the WRNS, two segments of bimodal volcanic and volcaniclastic rocks are collectively referred to as the NSA (Figures GS2018-5-1, 2a, b, c). The northern

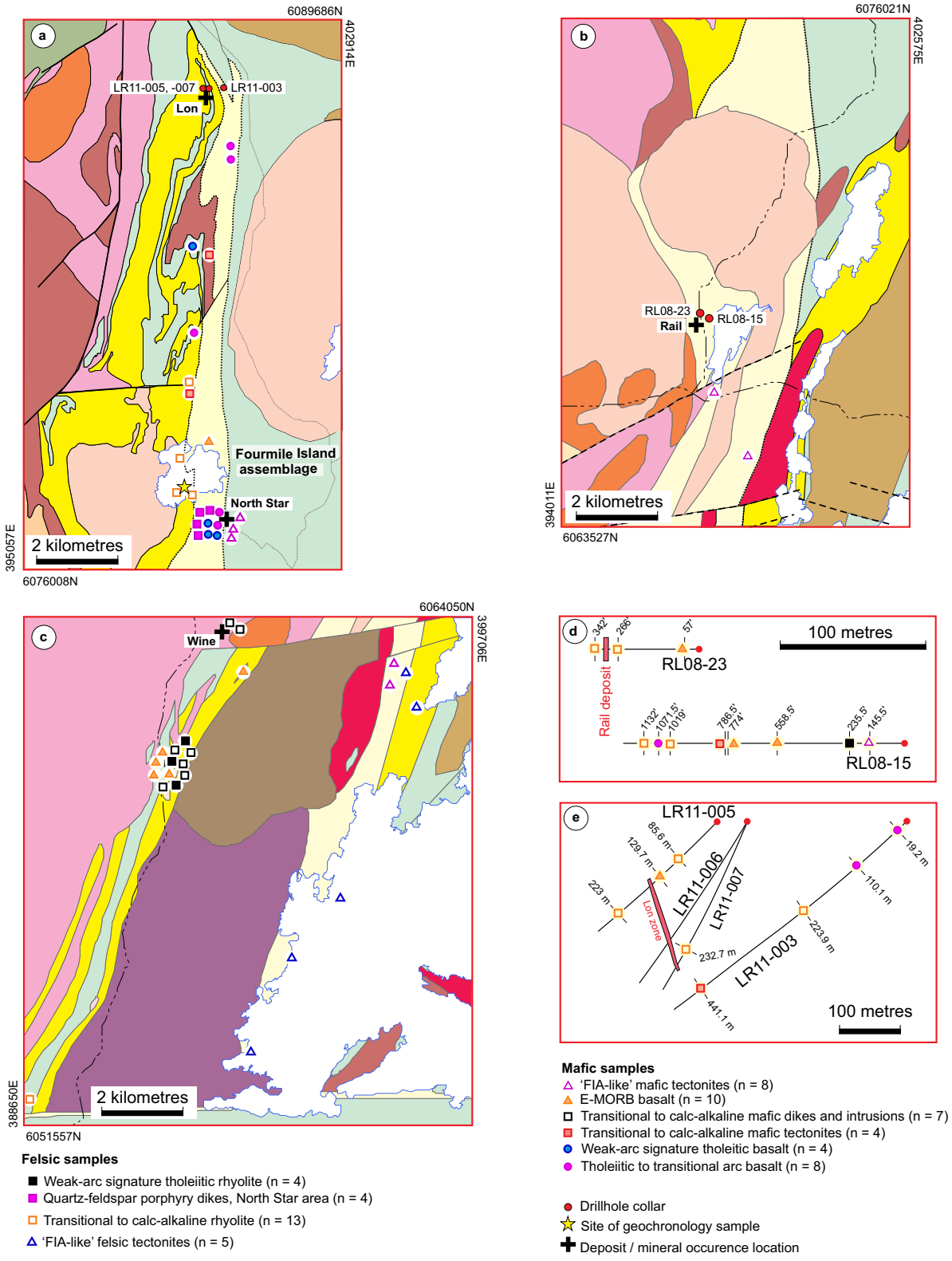

Figure GS2018-5-2: *Detailed geology of the three focus areas of the Flin Flon belt presented in this report, showing sample locations in* ***a)*** *the northern segment of the North Star assemblage (NSA);* ***b)*** *the Rail Lake area of the West Reed–North Star shear zone (WRNS);* ***c)*** *the southern segment of the NSA;* ***d)*** *the surface projection of the trace of two drillholes from the Rail deposit sampled by Simard et al. (2010), with sample locations indicated;* ***e)*** *an east-west vertical cross-section (looking north) along four drillholes that targeted the Lon volcanogenic massive sulphide deposit, with 2013 sample locations indicated. Geological units shown in a-c correspond to the legend in Figure GS2018-5-1. All NSA and WRNS geochemical samples are plotted on the map or along drillhole traces, with symbols reflecting their geochemical affinity.*

segment of the NSA extends northward from North Star Lake to southwest of Loonhead Lake over ~8 km and is host to the Lon VMS deposit (Figure GS2018-5-2a). The central portion of the WRNS is intruded by the Rail Lake pluton, lacks the less deformed NSA rocks along the western flank and is host to the Rail VMS deposit (Figure GS2018-5-2b). Figure GS2018-5-2c shows the southern portion of the NSA west of Reed Lake; Gagné and Anderson (2014a, b) described these rocks in detail. Detailed mapping and structural studies of the northern volcanic segment were conducted after the large 1989 Elbow Lake forest fire passed through the area. Detailed lithological descriptions and structural interpretations are provided in a series of Manitoba Geological Survey (MGS) Report of Activities (Norquay et al., 1991; Norquay et al., 1994) and a M.Sc. thesis (Norquay, 1997). However, no lithogeochemical analyses were published from these studies and very little work in terms of quantifying metamorphic petrology was done. These aspects are crucial to understanding the tectonometamorphic history of the supracrustal rocks of the NSA, and within the WRNS, and may provide vital information for assessing the mineral potential of the region.

This report provides the first geochemical characterization and Sm-Nd isotopic systematics of the rocks that form the NSA and the WRNS. In addition, the age of a rhyolite from the NSA is presented. New high-resolution geochemical data are presented here in combination with recent results from other MGS projects (Simard et al, 2010; Zwanzig and Bailes, 2010; Gagné and Anderson, 2014a) to provide a more comprehensive comparison. An update on metamorphic investigations in the North Star–Reed Lake–File Lake area, undertaken within the framework of a larger study of the metamorphism in the FFB conducted by M. Lazzarotto as part of his Ph.D. research at the University of Calgary (Lazzarotto et al., 2016, 2017), is presented in a companion paper (Lazzarotto et al., GS2018-6, this volume).

Regional geological framework

The exposed FFB contains several distinct juvenile-arc assemblages separated by major faults or intervening ocean-floor rocks, Burntwood group sedimentary rocks, plutonic rocks, or a combination of these. The volcanic assemblages are internally complex, commonly fault-bounded and folded, and typically bimodal suites (e.g., Bailes and Syme, 1989) with dominantly andesite/basalt and rhyolite/dacite flows, but also include a wide range of arc-related volcaniclastic and intrusive rocks (Bailes and Syme, 1989; Syme and Bailes, 1993; Stern et al., 1995a; Lucas et al., 1996; Bailes and Galley, 2007). The juvenile ocean-floor assemblages are composed mainly of mid-ocean–ridge basalt (MORB)–like basalt and related, layered, mafic–ultramafic plutonic complexes (Syme and Bailes, 1993; Stern et al., 1995b) that are kilometre-scale in width. Uranium-lead zircon ages for the ocean-floor assemblages in the exposed portion of the FFB indicate that ocean-floor magmatism was coeval with tholeiitic-arc volcanism around 1.9 Ga (Stern et al., 1995b).

The development of successor arcs resulted in the emplacement of voluminous plutons, coeval volcanism and deposition of sedimentary rocks. The successor-arc plutons were emplaced throughout the belt during three distinct magmatic stages (1878–1860 Ma, 1860–1844 Ma and 1843–1826 Ma; Whalen et al., 1999). Similar aged (ca. 1.88–1.83 Ga) volcanic, volcaniclastic and sedimentary rocks have been documented across the central and eastern parts of the exposed FFB and are interpreted as successor-basin deposits. They include the Schist–Wekusko assemblage, the Missi group and the Burntwood group. The fluvial–alluvial Missi group sedimentary deposits are characterized by thick packages of conglomerate, pebbly sandstone and massive sandstone. The marine turbidites of the Burntwood group include greywacke, siltstone, mudstone and rare conglomerate. In the low-grade metamorphic FFB, these sedimentary rocks are generally in fault contact with other units.

Exposed on the western shore of Reed Lake, the WRNS is a major, regionally extensive tectonite belt that lies between rocks of the FIA to the east and rocks of the NSA to the west (Figures GS2018-5-1, -2a–c). Collectively, rocks from the NSA, WRNS and FIA record a broad range of peak metamorphic conditions as discussed in Lazzarotto et al. (GS2018-6, this volume). For the sake of brevity, the prefix ‘meta-’ is not used in this report and the rocks are generally described in terms of their protoliths.

North Star assemblage

The NSA consists of two distinct segments, a northern and a southern segment (Figure GS2018-5-2a, c). According to Norquay (1997), the northern segment of the NSA (Figure GS2018-5-2a) comprises two intervals of rhyolitic rocks 600 and 100 m wide (Figure GS2018-5-3a) that host the Lon VMS deposit (Figure GS2018-5-3b, c). Two narrow successions of predominantly mafic volcanic rocks with lesser intermediate rock, minor siliciclastic intervals and iron formation are intercalated with the rhyolitic rocks and display a complex fold pattern. The felsic and mafic volcanic rocks of the northern segment of the NSA also include several zones of metamorphosed hydrothermal alteration exposed at surface

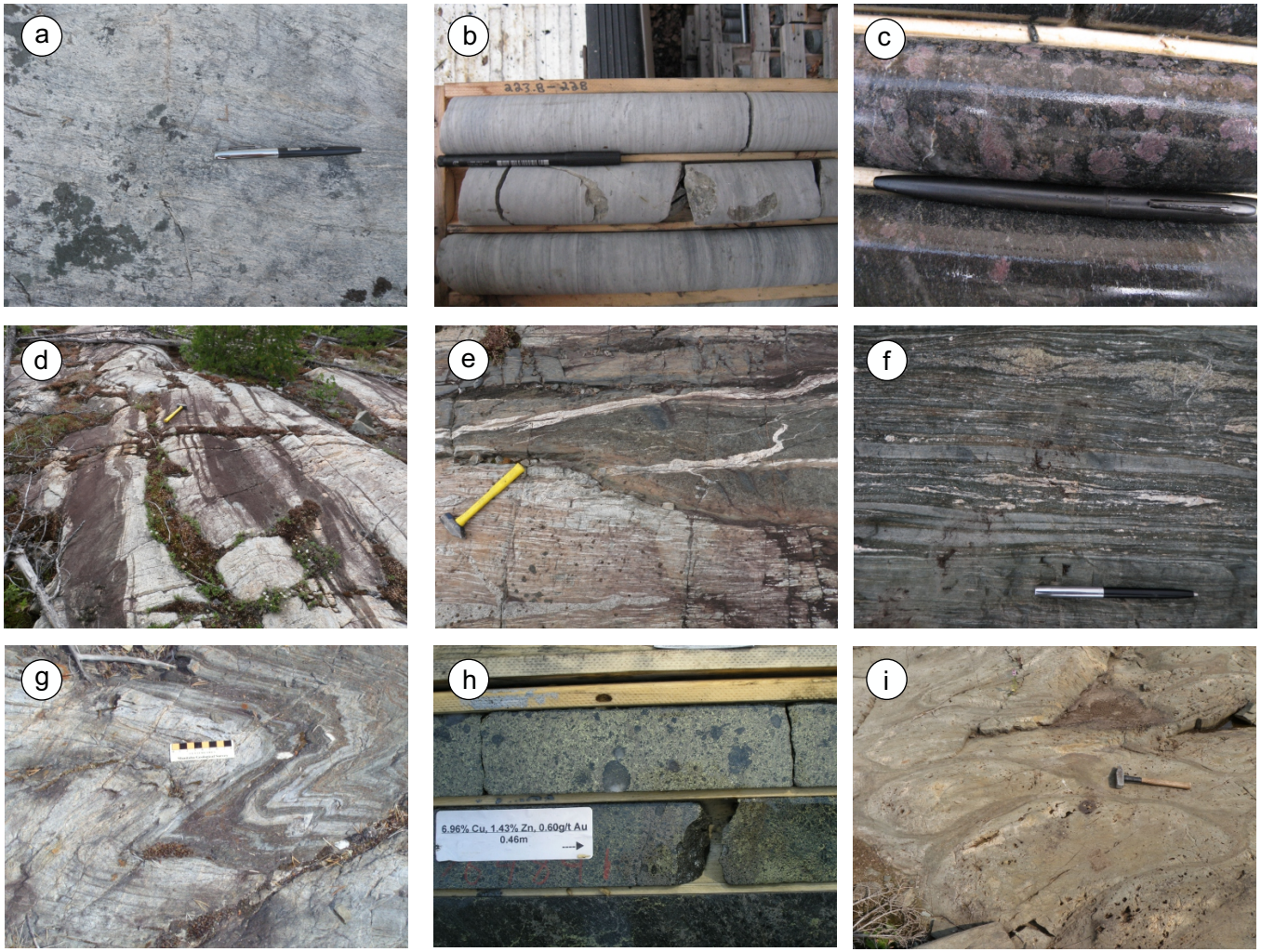

Figure GS2018-5-3: *Rock photographs showing* ***a)*** *strongly foliated, massive, homogeneous, quartz-phyric rhyolite of the northern North Star assemblage (NSA) segment on an island at North Star Lake (picture from sample 110-16-755 [399031E, 6077910N] analyzed for U-Pb geochronology);* ***b)*** *drillcore sample of rhyolite from the Lon deposit (LR-11-003 at 223 m; NQ core) in the northern NSA segment;* ***c)*** *drillcore sample of altered mafic gneiss containing abundant biotite and hornblende (black matrix minerals) with large garnet (pink) and staurolite (brown) porphyroblasts, from the Lon deposit (LR-11-003 at 85.3 m; NQ core) in the northern NSA segment;* ***d)****, rhyolite dikes in sparsely plagioclase-phyric basalt (392592E, 6060440N) from the southern NSA segment;* ***e)****, plagioclase-pyroxene–phyric dikes (dark coloured rocks) intruding felsic volcaniclastic rocks (392679E, 6061539N) from the southern NSA segment;* ***f)*** *mafic tectonites (400381E, 6073265N) from the West Reed–North Star assemblage (WRNS);* ***g)****, felsic tectonites interpreted as felsic tuff breccia (left) and intermediate crystal tuff (399801E, 6077439N) from the WRNS near North Star Lake;* ***h)*** *pyrrhotite-chalcopyrite solid sulphide horizons from diamond drill hole RL-08-23 at 93 m (NQ core) from the WRNS near the Rail deposit;* ***i)*** *large pillows from Preaston andesite (400381E, 6073265N) of the Fourmile Island assemblage. All co-ordinates are in UTM Zone 14 (NAD83). Drillcore diameter: NQ, 47.6 mm.*

and defined by the appearance or increasing abundance of porphyroblastic minerals, such as kyanite, staurolite, garnet and gahnite (Figure GS2018-5-3c). The southern segment of the NSA forms a narrow belt, some 300 to 500 m wide, consisting mainly of basaltic volcaniclastic rocks with intervals of mafic and felsic flows, and volcaniclastic rocks (Figure GS-2018-5-3d). The southern segment of the NSA is characterized by abundant syn- and postvolcanic dikes ranging in composition from mafic to felsic (Figure GS-2018-5-3e). Synvolcanic dikes, which are typically porphyritic with an aphanitic to fine-grained groundmass, are strongly foliated and transposed (Gagné and Anderson, 2014a).

West Reed–North Star shear zone

Felsic and mafic tectonites that form the WRNS extend for a strike length of 38 km along the western side of the FIA. The shear zone expands up to 1 km in width south of North Star Lake. Intense fabric within the mafic tectonite makes protolith determination difficult (Figure GS-2018-5-3f); however, in lower strain domains, possible remnant pillow selvages indicate that the protolith for this unit was, at least locally, mafic flows. The WRNS tectonites also include minor horizons of highly deformed felsic rocks of unknown precursor (Figure GS-2018-5-3g). The Rail VMS deposit is interpreted as being hosted within the WRNS (Figure GS-2018-5-3h).

Fourmile Island assemblage

West of Morton Lake, the FIA is 1.8 km thick and includes mafic to felsic volcanic rocks (Figures GS2018-5-1). The Preaston andesite at the base (Figure GS2018-5-3i) is stratigraphically overlain by the Dickstone rhyolite and, in turn, the Storozuk volcanic rocks, which are dominated by basalt (GS2018-5-2a-c). The Preaston andesite is found between the Dickstone rhyolite (felsic volcanic-arc rocks that extend southward from the Dickstone mine; Figures GS2018-5-1, 2a, b) and the eastern margin of the WRNS. The Storozuk mafic volcanic rocks extend along the eastern side of the Dickstone rhyolite and the Loonhead Lake area. The relatively thin (<330 m, not shown in Figures GS2018-5-1, 2) volcaniclastic Yakymiw formation forms the top of this succession (Bailes, 1980).

The FIA rocks were intruded by a compositionally zoned and highly fractionated mafic sill 1 km thick. The sill, part of the Josland Lake suite (Bailes, 1980), displays extreme iron fractionation and was dated at 1886 ±3 Ma (Zwanzig et al., 2001). This age indicates that the FIA volcanic rocks are part of the ca. 1.89 Ga juvenile-arc volcanic rocks that host the bulk of the VMS deposits in the FFB. The FIA is currently interpreted as a back-arc rift succession formed at about 1.89 Ga during opening of an ocean basin (Zwanzig and Bailes, 2010).

Sampling procedure and analytical methods

In order to characterize the geochemistry of the supracrustal rocks of the NSA and the tectonites of the WRNS, a suite of representative rock samples was collected for lithogeochemical analysis. The variations in trace-element chemistry and Sm-Nd isotopic composition can provide useful insight into the potential sources and geodynamic settings of magmatic rocks, and thus constrain regional-scale tectonic and metallogenic models. Major and trace-element compositions of all analyzed samples are available in Data Repository Item DRI2018003[3].

Whole-rock geochemistry

Sixty-seven drillcore, surface and underground samples provide regional coverage of the representative lithological units found within the NSA and WRNS (Figure GS2018-5-2). Where possible, samples were collected from the least altered rocks, but some include slightly altered material. All samples were trimmed to remove weathered surfaces, joints and veinlets; some samples may contain rare amygdules. Pulps were produced at the MGS rock laboratory using an agate mill. The pulps were then analyzed using the 4Lithores analytical package by Activation Laboratories Ltd. (Ancaster, Ontario). Major and minor elements were analyzed by inductively coupled plasma–emission spectrometry, and trace and rare-earth elements (REE) were analyzed using inductively coupled plasma–mass spectrometry (ICP-MS).

Sm-Nd isotopic analysis

Eight samples were submitted for Sm-Nd isotope geochemical analysis to the Radiogenic Isotope Facility of the University of Alberta (Edmonton, Alberta). Sampling and initial processing procedures were the same as those used for the lithogeochemical samples. Processing and analysis for $^{143}Nd/^{144}Nd$ and $^{147}Sm/^{144}Nd$ isotopic ratios followed the chromatographic and mass-spectrometry procedures described by Unterschutz et al. (2002) and Schmidberger et al. (2007). Samarium and Nd isotopic compositions were determined by multicollector ICP-MS

[3] MGS Data Repository Item DRI2018003 containing the data or other information sources used to compile this report is available online to download free of charge at https://www.gov.mb.ca/iem/info/library/downloads/index.html, or on request from minesinfo@gov.mb.ca, or by contacting the Resource Centre, Manitoba Growth, Enterprise and Trade, 360–1395 Ellice Avenue, Winnipeg, Manitoba R3G 3P2, Canada.

using an in-house Nd isotope standard (Schmidberger et al., 2007). Chemical-processing blanks were <200 pg for Nd and Sm. Neodymium isotope data are presented relative to a $^{143}Nd/^{144}Nd$ value of 0.511850 for the La Jolla Nd reference standard. Neodymium depleted-mantle model ages (T_{DM}) were calculated for samples with $^{147}Sm/^{144}Nd$ <0.14 using the model of DePaolo (1981), and present-day depleted-mantle values of $^{147}Sm/^{144}Nd$ = 0.2137 and $^{143}Nd/^{144}Nd$ = 0.513163. All epsilon Nd values (εNd) were calculated at the known or inferred age of crystallization (i.e., initial εNd values). They are reported relative to a chondritic uniform reservoir with present-day values of $^{147}Sm/^{144}Nd$ = 0.1967 (Jacobsen, 1980) and $^{143}Nd/^{144}Nd$ = 0.512638 (Goldstein et al., 1984).

U-Pb geochronology

Uranium-lead dating of the North Star rhyolite was carried out at the Jack Satterly Geochronology Laboratory at the University of Toronto. Sample preparation and analytical protocols generally followed those described in Bamburak et al. (2016).

Geochemistry

Mafic rocks

Mafic volcanic and selected intrusive samples from the NSA and the WRNS display five distinct geochemical signatures (Figure GS2018-5-4). For reference, analyses of the Preaston andesite and basalt flows (part of the FIA) from near the WRNS have been compiled from Zwanzig and Bailes (2010) and include unpublished samples collected by Gagné in 2013. Scatterplots show individual Preaston samples, but shaded areas reflect the unit's compositional range in the spider diagrams (Figure GS2018-5-4). Zwanzig and Bailes (2010) and Gagné and Anderson (2014a) discuss the geochemistry of the Preaston andesite in detail.

'FIA-like' mafic tectonites

Eight mafic tectonite samples mostly from the eastern side of the WRNS plot as basalt and andesite of distinctly tholeiitic affinity; these overlap closely with the Preaston andesite and basalt and are thus referred to as 'FIA-like' mafic tectonites (Figures GS2018-5-2, 4a, b). Mafic tectonite samples display a slightly enriched heavy REE (HREE) profile with a small negative Eu anomaly on a chondrite-normalized trace-element diagram (Figure GS2018-5-4c). On a primitive mantle–normalized, incompatible trace-element diagram (Figure GS2018-5-4d), the mafic rocks display distinct negative Nb anomalies and are depleted with respect to Ti. On a ternary Th-(Hf/3)-(Nb/16) diagram the rocks show a volcanic-arc affinity (Figure GS2018-10-4g), and on a Th/Nb versus Nb/Y diagram (Figure GS2018-5-4h) the FIA and 'FIA-like' mafic tectonites plot outside of the range of values of the Flin Flon arc rocks as compiled by Stern et al. (1995a). Mafic tectonite samples from the eastern margin of the WRNS appear to have very similar trace-element compositions to the Preaston andesite (Zwanzig and Bailes, 2010), indicating that the eastern portion of the WRNS is made up of FIA rocks caught up in the shear zone.

E-MORB

Ten samples of basalt with a tholeiitic to transitional affinity have slightly enriched light rare-earth-element (LREE) profiles and are referred to as 'E-MORB' (Figure GS2018-5-4a–c). On a primitive mantle–normalized incompatible trace-element diagram (Figure GS2018-5-4d), the basalt has an almost flat profile with samples showing either a weak positive or a weak negative Th signature and a weak negative Nb anomaly. On a ternary Th-(Hf/3)-(Nb/16) diagram (Figure GS2018-5-4g), the samples plot mostly in the E-MORB field. On a Th/Nb versus Nb/Y diagram (Figure GS2018-5-4h), the 'E-MORB' samples plot outside of the range of values of the Flin Flon arc rocks as compiled by Stern et al. (1995a) and overlap slightly with the compositional fields of both the N-MORB and E-MORB. Similar Th/Nb ratios (slightly elevated with respect to MORB) have also been documented within basalt of the Northeast Reed ocean-floor assemblage (Syme and Bailes, 1996) as well as in some basalt members of the Elbow–Athapapuskow ocean-floor assemblage (Stern et al. 1995b). Stern et al. (1995b) interpret these ratios as a subduction signature, rather than the result of crustal contamination; such MORB-like basalt with weak arc signatures suggests affinities with modern back-arc basin basalt.

Weak-arc tholeiitic basalt

Four samples mainly from the area immediately west of the North Star gold deposit plot as basalt with tholeiitic affinity and are referred to as 'weak-arc tholeiitic basalt' (Figures GS2018-5-2a and GS2018-5-4a, b). These show relatively flat REE profiles on a chondrite-normalized trace-element diagram (Figure GS2018-5-4e). On a primitive mantle–normalized incompatible trace-element diagram (Figure GS2018-5-4f), the 'weak-arc tholeiitic basalt' samples show almost flat profiles with weak to moderate relative depletions of Nb, Zr, Ti, V and Sc. On a ternary Th-(Hf/3)-(Nb/16) diagram (Figure GS2018-5-4g), the samples plot strictly in the arc-basalt field. These four samples plot close to the field of

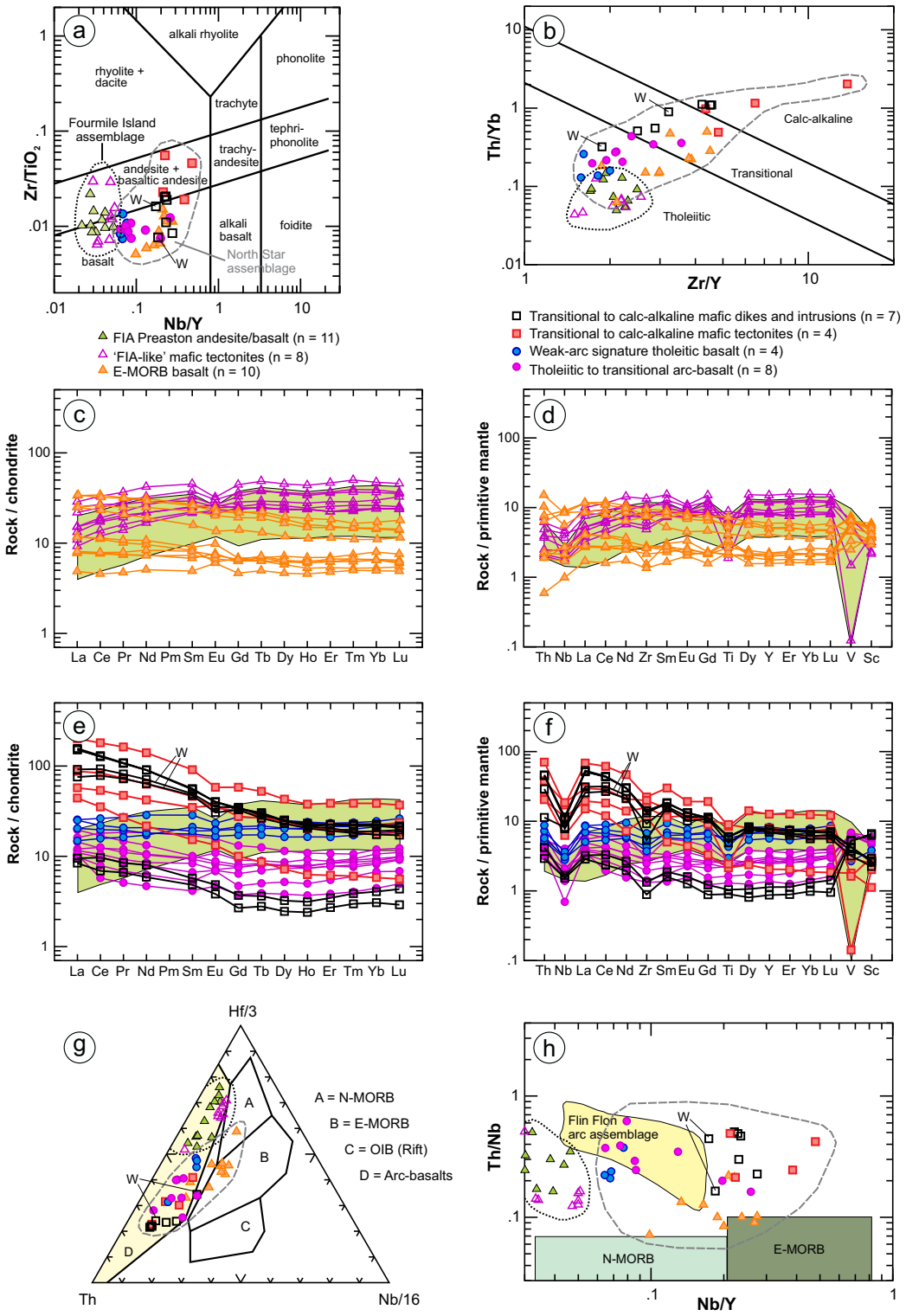

Figure GS2018-5-4: *Geochemical plots for mafic rocks of the North Star assemblage and West Reed–North Star shear zone areas:* ***a)*** *Zr/TiO_2 versus Nb/Y (modified from Winchester and Floyd, 1977);* ***b)*** *Th/ Yb versus Zr/Y (Ross and Bédard, 2009);* ***c)*** *and* ***e)*** *chondrite-normalized rare-earth element plots (normalizing values from McDonough and Sun, 1995);* ***d)*** *and* ***f)*** *primitive mantle–normalized incompatible trace-element plots (normalizing values from Sun and McDonough, 1989;* ***g)*** *Th-(Hf/3)-(Nb/16) ternary diagram after Wood (1980);* ***h)*** *Nb/Y versus Th/Nb discrimination diagram showing fields of primitive N-MORB and E-MORB (Saunders et al, 1988; Sun and McDonough, 1989), and Flin Flon assemblage arc rocks (from Stern et al., 1995a). Shaded areas in panels c–f indicate Preaston andesite compositions compiled from Zwanzig and Bailes (2010), and Gagné and Anderson (2014a). Abbreviations: E-MORB, enriched mid-ocean–ridge basalt; N-MORB, normal mid-ocean–ridge basalt; OIB, ocean-island basalt; W, Wine Ni-Cu-Co-PGE occurrence.*

the Flin Flon arc rocks on the Th/Nb versus Nb/Y diagram (Figure GS2018-5-4h).

Tholeiitic to transitional arc basalt

Eight samples, collected mostly from the northern NSA segment, are referred to as 'tholeiitic to transitional arc basalt' (Figure GS2018-5-2a). These plot as basaltic in the Zr/TiO_2 versus Nb/Y diagram (Figure GS2018-5-4a) and have a tholeiitic to transitional magmatic affinity (Figure GS2018-5-4b). The 'tholeiitic to transitional arc basalt' displays a slightly negative slope on a chondrite-normalized trace-element diagram (Figure GS2018-5-4e), with LREE enrichment and a flat to weak positive Eu anomaly. On a primitive mantle–normalized incompatible trace-element diagram (Figure GS2018-5-4f), the basalt samples show moderate negative Nb anomalies and positive V and Sc anomalies. On a ternary Th-(Hf/3)-(Nb/16) diagram (Figure GS2018-5-4g), the samples plot in the arc-basalt field. The 'tholeiitic to transitional arc basalt' samples plot mostly within the field of the Flin Flon arc rocks on the Th/Nb versus Nb/Y diagram (Figure GS2018-5-4h).

Transitional to calc-alkaline mafic rocks

Two subsets of samples, 'transitional to calc-alkaline mafic dikes and intrusions' and 'transitional to calc-alkaline mafic tectonites', have similar basaltic to andesitic composition based on the Zr/TiO_2 versus Nb/Y diagram (Figure GS2018-5-4a) and a transitional to calc-alkaline magmatic affinity (Figure GS2018-5-4b). The 'mafic dikes and intrusions' subset includes drillcore samples from the gabbro intrusion hosting the Wine Ni-Cu-Co-PGE occurrence (Figure GS2018-5-2c). These samples show strong LREE enrichment on a chondrite-normalized trace-element diagram (Figure GS2018-5-4e), with variation in overall enrichment interpreted as the result of magmatic differentiation from mafic to intermediate (49.4–65.0 SiO_2 wt. %). On a primitive mantle–normalized incompatible trace-element diagram (Figure GS2018-5-4f), the samples show strong negative slopes with strong negative Nb anomalies, moderate Zr depletions, flat to weakly depleted Ti, and variable V and Sc anomalies. On a ternary Th-(Hf/3)-(Nb/16) diagram (Figure GS2018-5-4g), the samples plot in the arc-basalt field. On the Th/Nb versus Nb/Y diagram (Figure GS2018-5-4h), these two subsets show higher ratios of Nb/Y than the FIA, NSA and Flin Flon arc rocks.

Felsic rocks

The geochemical characteristics of felsic supracrustal rocks from the NSA and the WRNS display three distinct geochemical signatures. For reference, a set of analyses including the Dickstone rhyolite (felsic flows from the FIA that lie closest to the WRNS) has been compiled from Zwanzig and Bailes (2010) and includes unpublished samples collected by Gagné in 2013. Scatterplots show individual Dickstone rhyolite samples, and the shaded areas reflect the unit's compositional range in the spider diagrams (Figure GS2018-5-5). Zwanzig and Bailes (2010) and Gagné and Anderson (2014a) discuss the geochemistry of the Dickstone rhyolite in detail.

'FIA-like' felsic tectonites

Samples of variably strained felsic tectonites from the eastern margin of the WRNS, 'FIA-like' felsic tectonites in Figure GS2018-5-2c and -5, plot in the rhyolite/dacite field on a Zr/TiO_2 versus Nb/Y diagram (Figure GS2018-5-5a) and have a tholeiitic magmatic affinity (Figure GS2018-5-5b). The rhyolite samples display slightly enriched HREE profiles, with weak negative Eu anomalies on a chondrite-normalized trace-element diagram (Figure GS2018-5-5c). On a primitive mantle–normalized incompatible trace-element diagram (Figure GS2018-5-5d), the samples display positive Th and negative Nb anomalies, and strongly depleted Ti. On a Nb versus Y discrimination diagram (Figure GS2018-5-5g), the felsic rocks all distinctly plot in the ocean-ridge field. The above-described geochemical characteristics are similar to the Dickstone rhyolite, indicating that the felsic tectonites along the eastern margin of the WRNS represent highly-strained FIA rocks entrained in the shear zone. On the La/Yb_{CN} versus Yb_{CN} diagram (Figure GS2018-5-5h), the 'FIA-like' felsic tectonites plot below the FIII rhyolite compositional range and show higher Yb_{CN} values than the FIV rhyolites from Hart et al (2004).

Weak-arc signature tholeiitic rhyolite

Four felsic samples from the southern segment of the NSA and the Rail deposit, referred to as 'weak-arc signature tholeiitic rhyolite', have a lower content of high-field-strength elements (HFSE), including Zr values of 30 to 49 ppm, and all plot in the andesite field on the Zr/TiO_2 versus Nb/Y diagram (Figure GS2018-5-2, -5a). Syme and Bailes (1993) and Bailes (1997) reported other examples of rhyolite that have similarly low HFSE content for the FFB. The samples all have a LOI (loss on ignition) of less than 1.2 wt. % and range from 70.9 to 78.9 wt. % SiO_2. The low-Zr rhyolite samples have a tholeiitic to transitional magmatic affinity (Figure GS2018-5-5b) and flat to slightly HREE-enriched chondrite-normalized profiles with flat to negative Eu anomalies (Figure GS2018-5-5c). Primitive mantle–normalized incompatible trace-element profiles have variable anomalies in Nb, Zr, Eu and

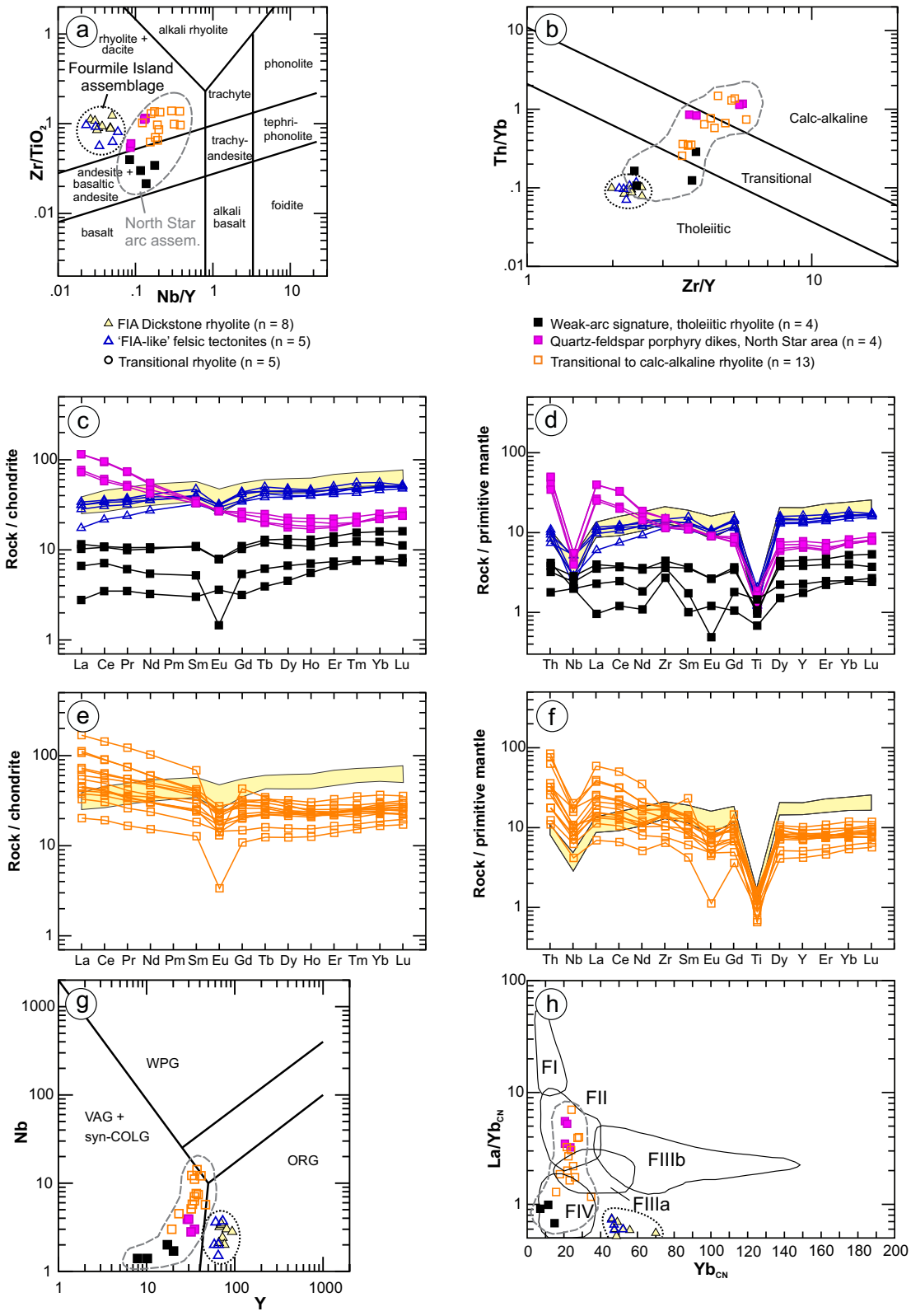

Figure GS2018-5-5: *Geochemical plots for felsic rocks of the North Star assemblage and West Reed–North Star shear zone areas:* ***a)*** *Zr/TiO_2 versus Nb/Y (modified from Winchester and Floyd, 1977);* ***b)*** *Th/ Yb versus Zr/Y (Ross and Bédard, 2009);* ***c)*** *and* ***e)*** *chondrite-normalized rare-earth-element plots (normalizing values from McDonough and Sun, 1995);* ***d)*** *and* ***f)*** *primitive mantle–normalized incompatible trace-element plots (normalizing values from Sun and McDonough, 1989;* ***g)*** *Nb versus Y (Pearce et al.,1984) and* ***h)*** *La/Yb_{CN} versus Yb_{CN} (Hart et al., 2004) discrimination diagrams. Shaded areas in panels c–f indicate Dickstone rhyolite compositional ranges compiled from Zwanzig and Bailes (2010), and Gagné and Anderson (2014a). Abbreviations: ORG, ocean-ridge granite; SynCOLG, syncollisional granite; VAG, volcanic-arc granite; WPG, within-plate granite.*

Ti (Figure GS2018-5-5d). The spread of data may be the result of synvolcanic alteration or metasomatic alteration during the development of the WRNS. The Nb versus Y diagram (Figure GS2018-5-5g) shows that the felsic rocks plot in the syncollisional volcanic-arc field. On the La/Yb_{CN} versus Yb_{CN} diagram (Figure GS2018-5-5h), the low-Zr rhyolite samples plot within the field of FIV rhyolite from Hart et al (2004).

Transitional to calc-alkaline rhyolite and quartz-feldspar porphyry dikes

Two sets of felsic samples share several geochemical characteristics, namely the 'transitional to calc-alkaline rhyolite' and 'quartz-feldspar porphyry dikes' (Figure GS2018-5-5). All samples plot as rhyolite/dacite (Figure GS2018-5-5a) and have a transitional to calc-alkaline magmatic affinity (Figure GS2018-5-5b). On a chondrite-normalized trace elements plot (Figure GS2018-5-5c, e), all samples display a similar negative slope. Many of the 'transitional to calc-alkaline rhyolite' samples show a moderate to strong negative Eu anomaly, unlike the porphyry dikes (Figure GS2018-5-5c, e). Primitive mantle–normalized incompatible trace elements show positive Th and negative Nb anomalies, and strong Ti depletion (Figure GS2018-5-5d, f). The samples plot in the syncollisional volcanic-arc field (Figure GS2018-5-5g). The rhyolite and porphyry dikes plot mostly in the FII and FIIIa field of Hart et al. (2004) on the La/Yb_{CN} versus Yb_{CN} diagram (Figure GS2018-5-5h).

Sm/Nd isotopes

Four rhyolite and three basalt samples from the NSA and WRNS were analyzed for Sm/Nd isotopes. The results span a narrow range of εNd values from +2.76 to 3.99 (Table GS2018-5-1), indicating that the rocks were derived from a juvenile-arc magma source. More specifically, they formed from depleted mantle in an oceanic environment or on recently evolved Paleoproterozoic crust with little or no influence of older (Archean) continental crust (Stern et al., 1995a, b; Whalen et al., 1999). These εNd values are distinctly lower than the published values of +4.61 and +6.72 for the Preaston andesite and the Dickstone rhyolite, respectively (Zwanzig and Bailes, 2010, Table 15).

U-Pb geochronology

Sample 110-16-755 (see Data Repository Item DRI-2018003), a sparsely quartz-phyric, massive, homogeneous and strongly foliated rhyolite from an island near the southern shore of North Star Lake (Figure GS2018-5-2a), was collected for U-Pb zircon age determination using isotope dilution–thermal ionization mass spectrometry at the Jack Satterly Geochronology Laboratory, University of Toronto.

Table GS2018-5-1: Samarium-neodymium isotope results for selected samples from the North Star assemblage and West Reed–North Star shear zone areas.

SAMPLE	UNIT	Geochemical grouping	LITHOLOGY	Nd ppm	Sm ppm	$^{147}Sm/^{144}Nd$	$^{143}Nd/^{144}Nd0$	UNCERT	TMA	εNdT
110-14-596-A01	North Star arc assemblage, northern segment	Transitional to calc-alkaline rhyolite	rhyolite	23.8	5.89	0.1495	0.51223	0.00001	1900	3.48
105-10-RL08-15-1019	North Star arc assemblage, Rail deposit area	Transitional rhyolite	Aphyric rhyolite	12.21	3.09	0.1528	0.5122	0.00001	1890	2.76
96-14-98-B1	North Star arc assemblage, southern segment	Low Zr rhyolite	rhyolite	5.12	1.67	0.1971	0.5128	0.00001	1890	3.98
105-10-RL08-15-235.5	North Star arc assemblage, Rail deposit area	Low Zr rhyolite	Qtz-phyric +/-chloritized rhyolite	4.54	1.51	0.2012	0.5129	0.00001	1890	3.99
105-10-RL08-15-1071.5	North Star arc assemblage, Rail deposit area	Tholeiitic to transitional arc-basalt	andesite, epidotized	4.62	1.26	0.1653	0.5124	0.00001	1890	3.07
105-10-RL08-15-558.5	North Star arc assemblage, Rail deposit area	E-MORB basalt	fine-grained andesite	14.07	3.89	0.1672	0.5125	0.00001	1890	3.52
96-14-92-A1	North Star arc assemblage, southern segment	E-MORB basalt	basalt	3.59	1.08	0.1827	0.5126	0.00001	1890	2.84

Several kilograms of rhyolite sample 110-16-755 yielded a modest amount of zircon, mostly elongated euhedral or subhedral, clear to cloudy, colourless crystals with length to breadth ratios of up to 4:1, but generally flat. The maximum dimension of the best quality grains is typically <200 μm, but rare, more clouded and altered grey grains reach up to ~300 μm (Figure GS2018-5-6a).

Four chemically abraded single zircon grain fractions were analyzed; U-Pb results are presented in Table GS2018-5-2 and displayed graphically in Figure GS2018-5-6b. Uranium concentrations in these fractions was relatively low, ranging from approximately 30–100 ppm, with Th/U ratios between 0.38 and 0.53. Most data overlap with or plot only slightly below concordia (0.5–1.6% discordant), yielding model $^{207}Pb/^{206}Pb$ ages between 1886–1896 Ma, although three of the fractions are colinear (Z1, Z2 and Z3) and give a weighted average $^{207}Pb/^{206}Pb$ age of 1895.9 ±1.6 Ma (2σ; mean square of weighted deviates [MSWD] = 0.25, probability of fit = 78%). A fourth fraction is displaced to the left of the main array of data and likely reflects minor secondary Pb loss. The age of 1895.9 ±1.6 Ma is interpreted to represent the primary age of eruption of the North Star rhyolite.

As reported in Stern et al. (1995b), juvenile-arc felsic volcanic rocks of the Flin Flon belt are difficult to date due to their low HFSE concentrations resulting in little zircon. As only a few rhyolite samples have been directly dated in the FFB, this newly obtained age of 1895.9 ±1.6 Ma for the North Star Lake rhyolite is significant. It confirms that the NSA represents a juvenile oceanic arc and that it formed around the time most VMS deposits of the FFB were produced. Recent geochronological results on four samples from the Flin Flon block by Rayner (2010) indicate that the bulk of the volcanism and associated VMS mineralization occurred ca. 1890 Ma. The significance of the 1903 +7/-5 Ma age from Stern et al. (1999, sample FF92-1) remains unclear. The timing of VMS mineralization in the Snow Lake arc assemblage is also ca. 1890 Ma. Two synvolcanic intrusions, the Richard Lake pluton and the Sneath Lake pluton, interpreted as the heat source for the VMS-hosting Anderson and Chisel sequences, have been respectively dated at 1886 +17/-9 Ma and at 1889 +8/-6 (Bailes et al., 1991; Bailes and Galley, 1999). The only U-Pb date from the host volcanic succession in the Snow Lake arc assemblage comes from a felsic volcaniclastic bed that provided a maximum age of 1892 +/-3 Ma (David et al., 1996) for the Anderson sequence.

Discussion

The geochemical data show that felsic and mafic volcanic rocks of similar geochemical signature occur both within the northern NSA segment and the southern NSA segment, indicating that both segments belong to the NSA (Figure GS2018-5-2a, c). The NSA has a trace-element geochemical signature that is distinct from the FIA but shares some features with the Flin Flon bimodal juvenile-arc sequences (Figures GS2018-5-4, -5). Further

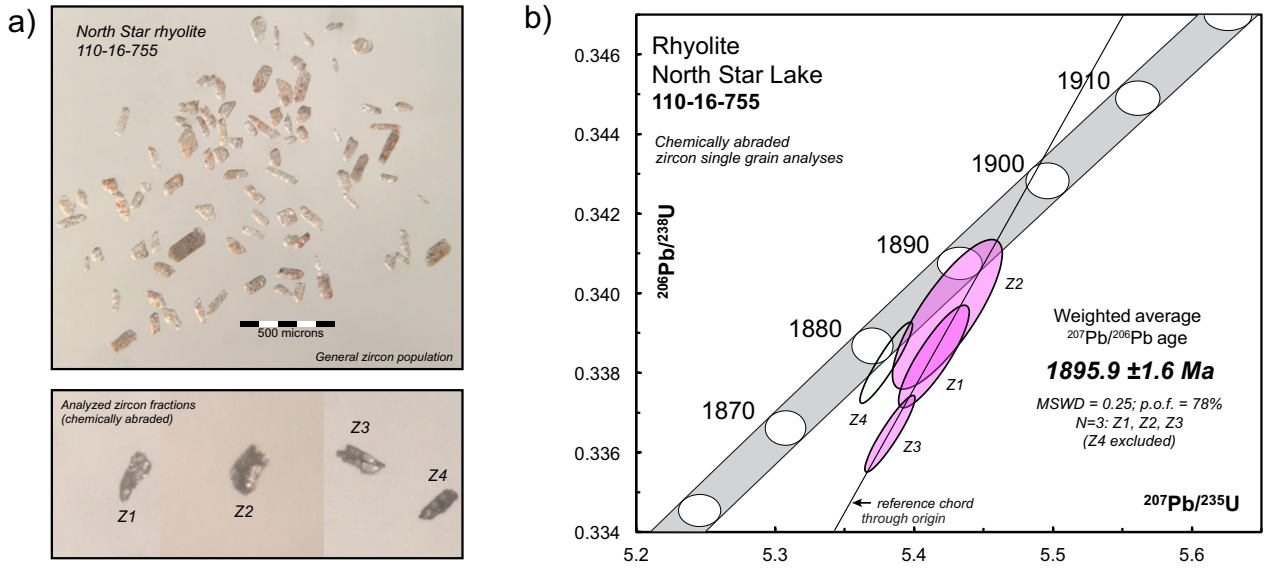

Figure GS2018-5-6: *Zircon grain images and concordia plots for rhyolite sample 110-16-755 (UTM Zone 14, 399031E, 6077910N [NAD83]) from the North Star Lake area:* ***a)*** *transmitted light photomicrographs of representative zircon grains; the lower image shows chemically abraded (annealed and etched) grain fragments selected for U-Pb analysis;* ***b)*** *concordia diagram showing U-Pb analytical results for zircon grains from rhyolite sample 110-16-755. Error ellipses are shown at the 2σ level of uncertainty. Calculated age shown is a weighted average of results for fractions Z1, Z2 and Z3 only; fraction Z4 (unshaded ellipse) is excluded. Concordia 'band' reflects uncertainties in U decay constants. Abbreviations: MSWD, mean square of weighted deviates; p.o.f., probability of fit.*

Table GS2018-5-2: Uranium-lead analytical results for zircon from a rhyolite sample from the North Star Lake area.

Sample Fraction	Description	Weight (mg)	U (ppm)	Th/U	Pb* (pg)	Pb_c (pg)	$^{206}Pb/^{204}Pb$	$^{206}Pb/^{238}U$	± 2σ	$^{207}Pb/^{235}U$	± 2σ	$^{207}Pb/^{206}Pb$	± 2σ
110-16-755 Rhyolite, North Star Lake													
Z1	1 cldy, cls, el frag	0.8	45	0.52	16.66	0.33	2957	0.33835	0.001060	5.41389	0.02055	0.11605	0.000225
Z2	1 cldy, cls brkn frag	1.1	27	0.38	9.51	0.40	1453	0.33941	0.001536	5.42345	0.03230	0.11589	0.000406
Z3	1 cldy and clr, cls,brkn el, crk	0.9	95	0.53	34.81	0.20	10377	0.33640	0.000785	5.38214	0.01467	0.11604	0.000124
Z4	1 dk grey, cldy el frag	0.7	69	0.44	24.95	0.21	7118	0.33819	0.000838	5.37972	0.01563	0.11537	0.000132

Sample Fraction	$^{206}Pb/^{238}U$ Age (Ma)	± 2σ	$^{207}Pb/^{235}U$ Age (Ma)	± 2σ	$^{207}Pb/^{206}Pb$ Age (Ma)	± 2σ	Disc. (%)
110-16-755 Rhyolite, North Star Lake							
Z1	1878.7	5.1	1887.1	3.3	1896.2	3.5	1.1
Z2	1883.8	7.4	1888.6	5.1	1893.8	6.3	0.6
Z3	1869.3	3.8	1882.0	2.3	1896.0	1.9	1.6
Z4	1878.0	4.0	1881.6	2.5	1885.7	2.1	0.5

Notes:
All analyzed fractions represent best quality zircon grains.
Abbreviations: brkn, broken; cldy, cloudy; clr, clear; cls, colourless; crk, cracked; dk, dark; el, elongated; frag, fragment.
Fraction weights (in micrograms) are estimated from digitally measured grain dimensions and the density of zircon (realistic errors are on the order of ± 20%)
Pb* is total amount (in picograms) of radiogenic Pb.
Pb_c is total measured common Pb (in picograms) assuming the isotopic composition of laboratory blank: $^{206/204}$ - 18.221; $^{207/204}$ - 15.612; $^{208/204}$ - 39.360 (errors of 2%).
Pb/U atomic ratios are corrected for spike, fractionation, blank, and, where necessary, initial common Pb; $^{206}Pb/^{204}Pb$ is corrected for spike and fractionation.
Th/U is model value calculated from radiogenic $^{208}Pb/^{206}Pb$ ratio and $^{207}Pb/^{206}Pb$ age assuming concordance.
Disc. (%) - per cent discordance for the given $^{207}Pb/^{206}Pb$ age.

geochemical sampling of the WRNS tectonites may allow to delineate more precisely the boundary between FIA rocks and NSA rocks.

Drillcore samples collected from the Rail deposit show the same geochemical character as the NSA rocks; the Rail deposit is therefore interpreted as belonging to the NSA. The rhyolite found within the host sequences of both the Rail and Lon VMS deposits (Figure GS2018-5-2d, e) are interpreted to be correlative to the North Star rhyolite; the deposits are interpreted to have formed around the time of crystallization of the North Star rhyolite at ca. 1896 Ma.

The presence of E-MORB, weak-arc tholeiites and bimodal transitional to calc-alkaline rocks within the NSA sequence suggests a complex magmatic history. The presence of E-MORB and the positive εNd values (+2.76–3.99; Table GS2018-5-1) indicates that the NSA was derived from a juvenile source, with magmatic contribution from an enriched mantle. Compared to the FIA, felsic samples from the NSA show depletions in HREE and lower Yb_{CN} and Y contents (Figure GS2018-5-5g, h), which is interpreted to suggest a deeper magmatic source for the NSA. However, other factors such as source composition and fractionation processes cannot be discounted given the available data.

Economic considerations

Base-metal potential

The recognition that the WRNS juxtaposes two packages of juvenile bimodal volcanic-arc sequences that host VMS and that these packages can be distinguished geochemically within the WRNS tectonites significantly expands the area prospective for base-metal mineralization. The shear zone itself should not be overlooked, given that the Rail deposit occurs in the western part of the WRNS and that this study demonstrates that the WRNS tectonites consist mostly of bimodal juvenile-arc volcanic rocks (host sequence characteristics that are broadly favourable for VMS mineralization; e.g., Syme and Bailes, 1993). In addition, the presence of prospective bimodal juvenile-arc rocks on the western margin of

the WRNS warrants further investigation along the full strike length of the structure.

Orogenic Au

The WRNS must represent a major crustal structure, as it separates two packages of arc rocks that have evolved in distinct tectonic environments. Such major crustal structures provide favourable pathways for deeply sourced, gold-bearing hydrothermal fluids and are prospective for orogenic gold mineralization. The WRNS is host to several significant Au showings in the North Star Lake area. Iron-enriched mafic rocks (such as the tholeiitic units found both in the FIA and NSA) near the WRNS may have served as a chemical trap for the sulfur-bearing fluids often associated with orogenic gold deposits (Dubé and Gosselin, 2007). The major structures associated with Au mineralization in the North Star Lake area extend southward to the Reed Lake area, which is considered to have similar potential for shear-hosted Au mineralization.

Magmatic Ni-Cu-Co-PGE mineralization

The Wine Ni-Cu-Co-PGE occurrence (Figure GS2018-5-2c) was discovered through drilling of a ground geophysical anomaly by Hudson Bay Exploration and Development Company Limited in the early 1980s. The mineralization is described as disseminated sulphides and stringers associated with a mafic magmatic breccia hosted by leucogabbro (Assessment Files 94660, 94667, 94669, Manitoba Growth, Enterprise and Trade, Winnipeg). Two samples collected from the gabbroic intrusion hosting the Wine occurrence display a transitional to calc-alkaline signature (Figure GS2018-5-4). Several other samples within the NSA and along the western margin of the WRNS share the same geochemical character (see 'transitional to calc-alkaline dikes and mafic intrusion' and 'transitional to calc-alkaline mafic tectonites' in Figure GS2018-5-4), which suggests that the western flank of the WRNS should be further tested for Ni-Cu-Co-PGE mineralization. Of particular interest is a folded gabbroic intrusion south of the Lon deposit, where one sample displayed a geochemical signature almost identical to that of the gabbro hosting the Wine occurrence. Three diabase/gabbro dike samples from the southern segment of the NSA also have the Wine gabbro geochemical signature.

Acknowledgments

The authors thank M. Rich, D. Campbell, S. Bawden, S. Kuschner, R. Green and R. Ponto for enthusiastic field assistance, as well as N. Brandson and E. Anderson for thorough logistical support. Thanks also go to K. Reid, C. Böhm and M. Rinne for reviewing this manuscript. They also thank G. Benger, V. Varga and C. Epp for their preparation of samples and thin sections.

References

Bailes, A.H. 1980: Geology of the File Lake area; Manitoba Energy and Mines, Mineral Resources Division, Geological Report GR78-1, 134 p.

Bailes, A.H. 1997: Geochemistry of Paleoproterozoic metavolcanic rocks in the Photo Lake area, Snow Lake, Flin Flon Belt; *in* Report of Activities 1997, Manitoba Energy and Mines, Geological Services, p. 61–72.

Bailes, A.H. and Galley, A.G. 1999: Evolution of the Paleoproterozoic Snow Lake arc assemblage and geodynamic setting for associated volcanic-hosted massive sulphide 88 deposits, Flin Flon Belt, Manitoba, Canada; Canadian Journal of Earth Science, v. 36, p. 1789–1805.

Bailes, A.H. and Galley, A.G. 2007: Geology of the Chisel–Anderson lakes area, Snow Lake, Manitoba (NTS areas 63K16SW and west half of 63J13SE); Manitoba Science, Technology, Energy and Mines, Manitoba Geological Survey, Geoscientific Map MAP2007-1, scale 1:20 000.

Bailes, A.H. and Syme, E.C. 1989: Geology of the Flin Flon–White Lake area; Manitoba Energy and Mines, Geological Services, Geological Report GR87-1, 313 p.

Bailes, A.H., Hunt, P.A. and Gordon, T.M. 1991: U-Pb zircon dating of possible synvolcanic plutons in the Flin Flon belt at Snow Lake, Manitoba; Radiogenic Age and Isotopic Studies: Report 4, Geological Survey of Canada, Paper 91-2, p. 35–43.

Bamburak, J.D., Hamilton, M. and Heaman, L.M. 2016: Geochronology of Late Cretaceous bentonite beds in southwestern Manitoba: 2016 update; *in* Report of Activities 2016, Manitoba Growth, Enterprise and Trade, Manitoba Geological Survey, p. 168–175.

David, J., Bailes, A.H. and Machado, N. 1996: Evolution of the Snow Lake portion of the Paleoproterozoic Flin Flon and Kisseynew belts, Trans-Hudson Orogen, Manitoba, Canada; Precambrian Research, v. 80, p. 107–124.

DePaolo, D.J. 1981: Neodymium isotopes in the Colorado Front Range and crust-mantle evolution in the Proterozoic; Nature, v. 291, p. 193–196.

Dubé, B. and Gosselin, P. 2007: Greenstone-hosted quartz-carbonate vein deposits; *in* Mineral Deposits of Canada: a Synthesis of Major Deposit-Types, District Metallogeny, the Evolution of Geological Provinces, and Exploration Methods, W.D. Goodfellow (ed.), Geological Association of Canada, Mineral Deposits Division, Special Publication no. 5, p. 49–73.

Gagné, S. 2013: Geological investigations in the Rail Lake–Sewell Lake area, Flin Flon–Snow Lake greenstone belt, west-central Manitoba (parts of NTS 63K10, 15); *in* Report of Activities 2013, Manitoba Mineral Resources, Manitoba Geological Survey, p. 95–105.

Gagné, S. 2017: Sub-Phanerozoic geology of the Reed Lake area, Flin Flon belt, west-central Manitoba (parts of NTS 63K7, 8, 9, 10); Manitoba Growth, Enterprise and Trade, Manitoba Geological Survey, Preliminary Map PMAP2017-2, scale 1:30 000.

Gagné, S. and Anderson, S.D. 2014a: Update on the geology and geochemistry of the west Reed Lake area, Flin Flon greenstone belt, west-central Manitoba (part of NTS 63K10); *in* Report of Activities 2014, Manitoba Mineral Resources, Manitoba Geological Survey, p. 77–93.

Gagné, S. and Anderson, S.D. 2014b: Bedrock geology west of Reed Lake, Flin Flon greenstone belt, Manitoba (part of NTS 63K10); Manitoba Mineral Resources, Manitoba Geological Survey, Preliminary Map PMAP2014-5, scale 1:20 000.

Gagné, S., Anderson, S.D., Hamilton, M., Simard, R.-L. and Lazzarotto, M. 2018: Geochemistry data of selected samples of volcanic and volcaniclastic rocks of the North Star assemblage, the West Reed–North Star shear zone and the Fourmile Island assemblage, Flin Flon belt, west-central Manitoba (parts of NTS 63K10, 15); Manitoba Growth, Enterprise and Trade, Manitoba Geological Survey, Data Repository Item DRI2018003, Excel® file.

Gagné, S., Syme, E.C., Anderson, S.D. and Bailes, A.H. 2017: Geology of the exposed basement in the Reed Lake area, Flin Flon belt, west-central Manitoba (parts of NTS 63K9, 10, 15, 16); Manitoba Growth, Enterprise and Trade, Manitoba Geological Survey, Preliminary Map PMAP2017-1, scale 1:30 000.

Goldstein, S.L., O'Nions, R.K. and Hamilton, P.J. 1984: A Sm-Nd study of atmospheric dusts and particulates from major river systems; Earth and Planetary Science Letters, v. 70, p. 221–236.

Hart, T.R., Gibson, H.L. and Lesher, C.M. 2004: Trace element geochemistry and petrogenesis of felsic volcanic rocks associated with volcanogenic massive Cu-Zn-Pb sulfide deposits; Economic Geology, v. 99, p. 1003–1013.

Jacobsen, S.B. 1980: Sm-Nd isotopic evolution of chondrites; Earth and Planetary Science Letters, v. 50, p. 139–155.

Lazzarotto, M., Gagné, S. and Pattison, D.R.M. 2016: Tectonometamorphic investigations in the Athapapuskow Lake area, west-central Manitoba (part of NTS 63K12); *in* Report of Activities 2016, Manitoba Growth, Enterprise and Trade, Manitoba Geological Survey, p. 87–98.

Lazzarotto, M., Pattison, D.R.M. and Gagné, S. 2017: Prehnite-pumpellyite– to amphibolite-facies metamorphism in the Athapapuskow Lake area, west-central Manitoba (parts of NTS 63K12, 13); *in* Report of Activities 2017, Manitoba Growth, Enterprise and Trade, Manitoba Geological Survey, p. 104–116.

Lucas, S.B., Stern, R.A., Syme, E.C., Reilly, B.A. and Thomas, D.J. 1996: Intraoceanic tectonics and the development of continental crust; 1.92–1.84 Ga evolution of the Flin Flon Belt, Canada; Geological Society of America Bulletin, v. 108, no. 5, p. 602–629.

McDonough, W.F. and Sun, S.-S. 1995: The composition of the Earth; *in* Chemical Evolution of the Mantle, W.F. McDonough, N.T. Arndt and S. Shirey (ed.), Chemical Geology, v. 120, p. 223–253.

NATMAP Shield Margin Project Working Group 1998: Geology, NATMAP Shield Margin Project area, Flin Flon belt, Manitoba/Saskatchewan; Geological Survey of Canada, Map 1968A, scale 1:100 000.

Norquay, L.I. 1997: Structural and metamorphic evolution of the North Star Lake area, Manitoba; M.Sc. thesis, University of Manitoba, 244 p.Norquay. L.I., Prouse, D.E., Bieri, M. and Gale, G.H. 1991: Geology of a part of the North Star Lake area (NTS 63K/15); *in* Report of Activities 1991, Manitoba Energy and Mines, Minerals Division, p. 31–40.

Norquay, L.I., Prouse, D.E. and Gale., G.H. 1994: The North Star Lake project (NTS 63K/15); *in* Report of Activities 1994, Manitoba Energy and Mines, Minerals Division, p. 83–84.

Pearce, J.A., Harris, N.B.W. and Tindle, A.G. 1984: Trace element discrimination diagrams for the tectonic interpretation of granitic rocks; Journal of Petrology, v. 25, p. 956–983.

Rayner, N.M. 2010: New U-Pb zircon ages from the Flin Flon Targeted Geoscience Initiative Project 2006-2009: Flin Flon and Hook Lake blocks, Manitoba and Saskatchewan, Geological Survey of Canada, Current Research (Online) no. 2010-4, 12 p., doi:10.4095/261489

Ross, P.-S. and Bédard, J.H. 2009: Magmatic affinity of modern and ancient sub-alkaline volcanic rocks determined from trace-element discriminant diagrams; Canadian Journal of Earth Sciences, v. 46, p. 823–839.

Saunders, A.D., Norry, M.J. and Tarney, J. 1988: Origin of MORB and chemically-depleted mantle reservoirs: trace element constraints; Journal of Petrology, Special Volume 1, p. 415–445.

Schmidberger, S.S., Heaman, L.M., Simonetti, A., Creaser, R.A. and Whiteford, S. 2007: Lu-Hf, in-situ Sr and Pb isotope and trace element systematics for mantle eclogites from the Diavik diamond mine: evidence for Paleoproterozoic subduction beneath the Slave craton, Canada; Earth and Planetary Science Letters, v. 254, p. 55–68.

Simard, R.-L., McGregor, C.R., Rayner, N. and Creaser, R.A. 2010: New geological mapping, geochemical, Sm-Nd isotopic and U-Pb age data for the eastern sub-Phanerozoic Flin Flon Belt, west-central Manitoba (parts of NTS 63J3–6, 11, 12, 14, 63K1–2, 7–10); *in* Report of Activities 2010, Manitoba Innovation, Energy and Mines, Manitoba Geological Survey, p. 69–87.

Stern, R.A., Machado, N., Syme, E.C., Lucas, S.B. and David, J. 1999: Chronology of crustal growth and recycling in the Paleoproterozoic Amisk collage (Flin Flon Belt), Trans-Hudson Orogen, Canada; Canadian Journal of Earth Sciences, v. 36, p. 1807–1827.

Stern, R.A., Syme, E.C., Bailes, A.H. and Lucas, S.B. 1995a: Paleoproterozoic (1.90–1.86 Ga) arc volcanism in the Flin Flon Belt, Trans-Hudson Orogen, Canada; Contributions to Mineralogy and Petrology, v. 119, no. 2–3, p. 117–141.

Stern, R.A., Syme, E.C. and Lucas, S.B. 1995b: Geochemistry of 1.9 Ga MORB- and OIB-like basalts from the Amisk collage, Flin Flon Belt, Canada: evidence for an intra-oceanic origin; Geochimica et Cosmochimica Acta, v. 59, no. 15, p. 3131–3154.

Sun, S.-S. and McDonough, W.F. 1989: Chemical and isotopic systematics of oceanic basalts: implication for mantle composition and processes; The Geological Society of London, Special Publications, v. 42, p. 313–345.

Syme, E.C. and Bailes, A.H. 1993: Stratigraphic and tectonic setting of early Proterozoic volcanogenic massive sulfide deposits, Flin Flon, Manitoba; Economic Geology, v. 88, no. 3, p. 566–589.

Syme, E.C. and Bailes, A.H. 1996: Geochemistry of arc and ocean-floor metavolcanic rocks in the Reed Lake area, Flin Flon belt; *in* Report of Activities 1996, Manitoba Energy and Mines, Geological Services, p. 52–65.

Syme, E.C., Bailes, A.H. and Lucas, S.B. 1995a: Reed Lake, parts of NTS 63K/9, 63K/10; Manitoba Energy and Mines, Geological Services, Preliminary Map 1995F-1, scale 1:50 000.

Syme, E.C., Bailes, A.H. and Lucas, S.B. 1995b: Geology of the Reed Lake area (parts of NTS 63K/9 and 10); *in* Report of Activities 1995, Manitoba Energy and Mines, Geological Services, p. 42–60.

Syme, E.C., Lucas, S.B., Bailes, A.H. and Stern, R.A. 1999: Contrasting arc and MORB-like assemblages in the Paleoproterozoic Flin Flon Belt, Manitoba, and the role of intra-arc extension in localizing volcanic-hosted massive sulphide deposits; Canadian Journal of Earth Sciences, v. 36, p. 1767–1788.

Unterschutz, J.L.E., Creaser, R.A., Erdmer, P., Thompson, R.I. and Daughtry, K.L. 2002: North American margin origin of Quesnel terrane strata in the southern Canadian Cordillera: inferences from geochemical and Nd isotopic characteristics of Triassic metasedimentary rocks; Geological Society of America Bulletin, v. 114, p. 462–475.

Whalen, J.B., Syme, E.C. and Stern, R.A. 1999: Geochemical and Nd isotopic evolution of Paleoproterozoic arc-type granitoid magmatism in the Flin Flon Belt, Trans-Hudson Orogen, Canada; Canadian Journal of Earth Sciences, v. 36, p. 227–250.

Winchester, J.A. and Floyd, P.A. 1977: Geochemical discrimination of different magma series and their differentiation products using immobile elements; Chemical Geology, v. 20, no. 4, p. 325–343.

Wood, D.A. 1980: The application of a Th-Hf-Ta diagram to problems of tectonomagmatic classification and to establishing the nature of crustal contamination of basaltic lavas of the British Tertiary volcanic province; Earth and Planetary Science Letters, v. 50, p. 11–30.

Zwanzig, H.V. and Bailes, A.H. 2010: Geology and geochemical evolution of the northern Flin Flon and southern Kisseynew domains, Kississing–File lakes area, Manitoba (parts of NTS 63K, N); Manitoba Innovation, Energy and Mines, Manitoba Geological Survey, Geoscientific Report GR2010-1, 135 p.

Zwanzig, H.V., Bailes, A.H. and Böhm, C.O. 2001: Josland Lake Sills: U-Pb age and tectonostratigraphic implications (parts of NTS 63K and 63N); *in* Report of Activities 2001, Manitoba Industry, Trade and Mines, Manitoba Geological Survey, p. 28–32.